

Hisashi Nakamura^{*1,2}, Takeaki Sampe¹, Youichi Tanimoto^{2,3}, Akihiko Shimpo⁴, Wataru Ohfuchi⁵,
and Shang-Ping Xie⁶

¹Department of Earth and Planetary Science, University of Tokyo, Tokyo, JAPAN;

²Frontier Research Center for Global Change, Yokohama, JAPAN;

³Graduate School of Environmental Earth Science, Hokkaido University, Sapporo, JAPAN;

⁴Climate Prediction Division, Japan Meteorological Agency, Tokyo, JAPAN;

⁵Earth Simulator Center, Yokohama, JAPAN;

⁶International Pacific Research Center, University of Hawaii, Honolulu, HI, U.S.A.

1. INTRODUCTION

Synoptic-scale baroclinic eddies migrating along mid-latitude storm tracks not only influence daily weather but also play a crucial role in the climate system by systematically transporting heat, moisture and angular momentum. As reviewed by Chang et al. (2002), recent studies have substantiated a notion of downstream development, in recognition of group-velocity propagation of synoptic-scale eddies along storm tracks (Lee and Held 1993; Chang 1993, 1999; Swanson and Pierrehumbert 1994; Orlanski and Chang 1995; Berbery and Vera 1996; Chang and Yu 1999). In "PV thinking" (Hoskins et al. 1985), baroclinic eddy growth is interpreted as mutual reinforcement between PV anomalies at the tropopause and those in the form of temperature anomalies at the surface. In the downstream development, the thermal anomalies are triggered by wind fluctuations across a surface baroclinic zone induced by a propagating upper-level vortex. Thus, surface temperature gradient is of particular significance in baroclinic instability. Nevertheless, in most of the studies from the wave dynamic perspective, storm tracks have been regarded as a pure atmospheric issue.

Forecast experiments have shown the importance of heat and moisture supply from the warm ocean surface of the Kuroshio or Gulf Stream in individual events of rapid cyclone development. A regional-model experiment by Xie et al. (2002) indicates that cyclone development is sensitive to a fine frontal structure in a sea-surface temperature (SST) field between the Kuroshio and shallow East China Sea. Climatologically, rapid cyclone development over the Northern Hemisphere (NH) is most likely along the Gulf Stream and Kuroshio (Sanders and Gyakum 1980). Over the Southern Hemi-

sphere (SH), maritime cyclogenesis is most frequent around an intense oceanic frontal zone in the Indian Ocean (Sinclair 1995). These observational tendencies suggest the oceanic influence on storm track formation. At the same time, storm tracks can in turn influence the underlying ocean. By means mainly of their poleward heat flux, eddies migrating along a storm track transfer mean-flow westerly momentum downward, acting to sustain surface westerlies (Lau and Holopainen 1984). In fact, Hoskins and Valdes (1990, hereafter HV90) considered a storm track could be self-maintained under the heat and moisture supply from a nearby warm ocean current that is driven by the eddy-maintained surface westerlies. Those eddies also supply fresh water to the ocean, influencing the stratification in the midlatitude upper ocean (Lukas 2001).

The main purpose of this paper is to further discuss the importance of the atmosphere-ocean coupling via storm tracks in the tropospheric circulation system and its long-term variability from the wave dynamic viewpoint, based on observational statistics. Our argument may be viewed as an extension of HV90, but unlike in HV90, we put emphasis on oceanic frontal zones associated with major oceanic currents. As the surface air temperature over the open ocean is linked to SST underneath, maritime surface baroclinic zones tend to be anchored along oceanic frontal zones (Nakamura and Shimpo 2004; hereafter NS04). Though acting as thermal damping for the evolution of individual eddies, heat exchange with the underlying ocean, on longer time scales, can act to restore atmospheric near-surface baroclinicity against the relaxing effect by atmospheric eddy heat transport, as evident in sharp meridional contrasts in upward turbulent heat fluxes observed climatologically across midlatitude frontal. In section 2, we discuss associations among storm tracks, polar-frontal (or subpolar) jet streams and underlying oceanic frontal

* Corresponding author address: Hisashi Nakamura, Dept. of Earth & Planetary Science, Univ. of Tokyo, Tokyo, 113-0033, JAPAN; e-mail: hisashi@eps.s.u-tokyo.ac.jp

zones over the two hemispheres. In section 3, we then discuss how such an association can be disturbed in winter by the intensification of a subtropical jet stream. Finally, we propose a working hypothesis through which our understanding might be deepened on the observed tropospheric circulation system and its variability. More details can be found in Nakamura et al. (2004).

2. ASSOCIATIONS AMONG STORM TRACKS, POLAR-FRONT JETS AND OCEANIC FRONTS

a. Southern Hemisphere (SH)

Figure 1 shows the SH climatology of storm track activity, westerly wind speed and SST gradient. A prototype example of a close association among a subarctic frontal zone, midlatitude storm track and polar-front jet can be found around 50°S especially in austral summer (Figs. 1d-f; NS04). In winter, the association is still close over the South Atlantic and Indian Ocean (Figs. 1a-c). There the low-level storm track activity is stronger than over the South Pacific, which seems in correspondence with tighter SST gradient across the Antarctic Polar Frontal Zone (APFZ; Colling 2001), a subarctic frontal

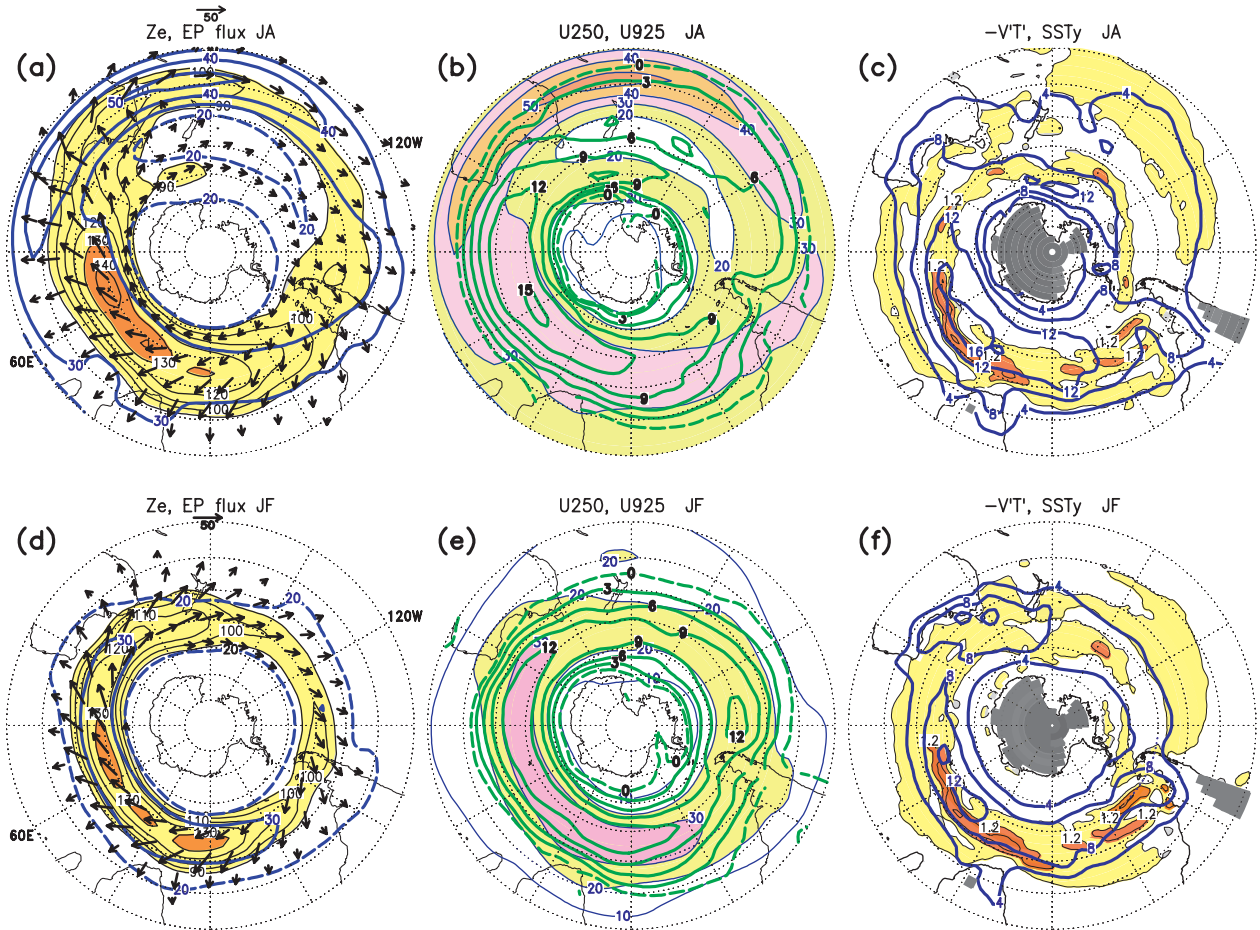


Figure 1. (a) Climatological Jul.-Aug. distribution for the upper-level SH storm track activity (colored) and horizontal component of 250-hPa extended E-P flux (arrows indicating eddy transport of mean-flow easterly momentum; scaling at the top: unit: $m^2 s^{-2}$), with 250-hPa westerly wind speed (U : $m s^{-1}$; blue solid lines for 30, 40, 50 and 60; blue dashed line for 20). Yellow and orange coloring denotes amplitude of subweekly fluctuations in 250-hPa height (Z_e : m) is between 90 and 130 and above 130, respectively, with thin lines for every 10. Based on the NCEP/NCAR reanalyses. (b) As in (a) but for 925-hPa U ($m s^{-1}$; green lines for 3, 6, 9, 12 and 15; dashed for $U = 0$) and 250-hPa U ($m s^{-1}$; yellow: 20~30; pink: 30~40; orange: 40~50; red: 50~60). (c): As in (a), but for 850-hPa poleward heat flux associated with subweekly eddies (blue lines for 4, 8, 12 and 16 $K m s^{-1}$). Yellow and orange coloring indicates oceanic frontal zones where meridional SST gradient ($^{\circ}C/110 km$) exceeds 0.6 and 1.2, respectively (thin lines are drawn for every 0.6), based on satellite and shipboard data compiled by Reynolds and Smith (1994). Dark shading indicates data-void regions. (d-f) As in (a-c), respectively, but for Jan.-Feb. After NS04 and Nakamura et al. (2004).

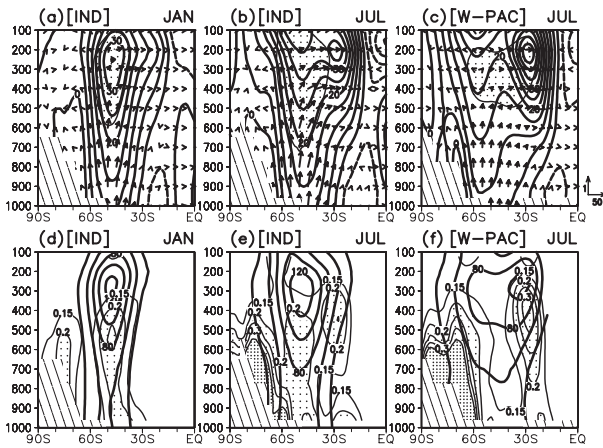


Figure 2. (a) Climatological Jan. section of meridional ($\text{m}^2 \text{s}^{-2}$) and vertical (Pa m s^{-2} ; proportional to poleward eddy heat flux) components of the extended E-P flux (arrows; scaling at the lower-right corner), and U (contoured for every 5 m s^{-1} ; dashed for easterlies), both for the South Indian Ocean ($50^\circ\sim 90^\circ\text{E}$). Based on the NCEP reanalyses. (b) As in (a) but for July. (c) As in (a) but for July in the Australian sector ($120^\circ\sim 160^\circ\text{E}$). Hatching indicates topography. (d-f) As in (a-c), respectively, but for eddy amplitude in geopotential height (Z_e ; unit: m; heavy lines for every 20 from 40) and local baroclinicity (G ; thin lines for every 0.05 from 0.15; light stippling for 0.2~0.35 and heavy stippling for above 0.35). Here, $G = |g/f_0| \cdot |\nabla\theta|/(\theta N)$, where N is the Brunt-Väisälä frequency, θ potential temperature, g acceleration of gravity, f the Coriolis parameter and $f_0 = f(45^\circ\text{S})$. In linear theories of baroclinic instability for zonally uniform westerlies, the maximum growth rate of the most unstable mode is proportional to G . In (a-c), stippling for $Z_e > 80$ (m). After NS04.

zone along the Antarctic Circumpolar Current (ACC), over the former oceans. Along that frontal zone, a strong baroclinic zone forms near the surface (Figs. 2d-e). Both in the upper and lower troposphere (Fig. 1), the storm track core forms in the southwestern Indian Ocean, almost coinciding with the core of the APFZ. In fact, Sinclair (1995) found that the most frequent cyclogenesis in the SH occurs around this APFZ core. There, in the course of the seasonal march, the low-level storm track activity exhibits high positive correlation with baroclinicity for a layer just above the surface. NS04 showed that the correlation is even higher than that with the baroclinicity near the steering (700~850 hPa) level of subweekly eddies, which is also the case for the South Atlantic. Meridional sections in Figs. 2d-e show a deep structure of the storm track over the Atlantic and Indian Ocean. The structure reflects the pronounced baroclinic eddy growth above the intense surface baroclinic zone and the downstream development of eddies along the upper-level polar-front jet that acts as a good waveguide for baroclinic wave packets (Figs. 2a-b). In fact, the extended Eliassen-Palm (E-P) flux has a strong eastward component in the core of the upper-level storm track (NS04). The jet is the sole westerly jet in summer. Even in winter when a subtropical jet intensifies, the storm track core over the South Indian Ocean remains preferentially along the polar-front jet (Fig. 1).

The SH storm track core is collocated with the core of the surface westerly jet (Fig. 1) as part of the deep polar-front jet (Figs. 2a-b) maintained mainly by the downward transport of mean-flow westerly momentum via eddy heat fluxes. The fact that the strongest annual-mean wind stress within the world ocean is observed around the SH storm core (Trenberth et al. 1990) suggests the importance of the storm track activity in driving the ACC and associated APFZ. As shown in Fig. 3, the annually averaged surface westerly acceleration in-

duced as the feedback forcing through heat and vorticity transport by subweekly eddies is indeed strong along or slightly poleward of the surface westerly axis, and it is strongest near the core of the APFZ. The slight poleward displacement of that axis relative to the APFZ (Fig. 1) seems consistent with a tendency for surface upward turbulent heat fluxes, wind stirring effect on the oceanic mixed layer, and Ekman velocity to be all maximized along the wind velocity axis. Consistent with an evaluation by Lau and Holopainen (1984) for the NH, a contribution from eddy heat transport is stronger than that from eddy vorticity transport, but their contributions are more comparable (not shown).

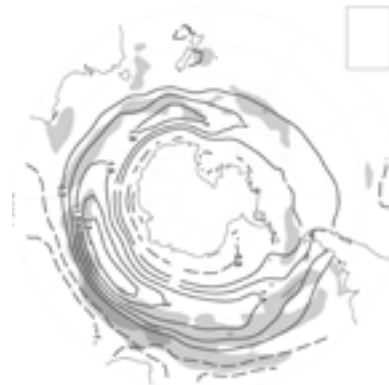


Figure 3. Climatological annual-mean westerly acceleration (solid lines at $0.5 \text{ m s}^{-1}/\text{day}$ intervals with zero lines omitted; dashed lines for easterly acceleration) at the 1000-hPa level over the SH, as the feedback forcing from storm tracks evaluated in the same manner as in Lau and Holopainen (1984) but based on 8-day high-pass-filtered NCEP reanalysis data for 1979~98. Light and heavy stippling indicates oceanic frontal zones where climatological annual-mean meridional SST gradient ($^\circ\text{C}/110 \text{ km}$) is 0.8~1.6 and above 1.6, respectively, based on the data by Reynolds and Smith (1994).

Over the South Pacific, the association among a mid-latitude storm track, polar-front jet and subarctic frontal zone is less robust than over the Atlantic and Indian Ocean (NS04). Though vulnerable to the seasonal intensification of a subtropical jet, their close association can still be found in austral summer and autumn when the jet is diminished. In these seasons, the Pacific storm track at the upper and lower levels is part of a well-defined circumpolar storm track along the $\sim 50^\circ\text{S}$ circle, accompanied consistently by the deep polar-front jet (Figs. 1d-f). The low-level eddy activity gradually weakens downstream across the Pacific, as the SST gradient relaxes eastward along the APFZ (Fig. 1f). The close association was observed also in a very unusual winter at the beginning of the 1998 La Niña event, in the absence of the intense subtropical jet due to the marked interannual variability. In that winter, the upper-level westerly bifurcation was much less apparent than in the climatology, which marks a sharp contrast with a distinct double-jet structure in the previous winter, as in other El Niño winters (Chen et al. 1996). As well inferred from a difference map in Fig. 4a, no well-defined storm track formed over the subtropical South Pacific in the 1998 winter, under the extremely weakened subtropical jet. Instead, eddy activity over the South Pacific was enhanced at midlatitudes and organized into a single storm track along the polar-front jet at $\sim 55^\circ\text{S}$ throughout the troposphere (Fig. 4), which indeed resembled the summertime situation (Fig. 2). In 1998, the midlatitude westerlies were stronger not only in the upper troposphere but also near the surface (Fig. 4), consistent with coherent vertical structure of the midlatitude storm track. In that winter, upper-level wave activity was dispersed strongly equatorward from the enhanced subpolar storm track in the central and eastern Pacific, through which the westerly momentum was transported poleward. Its downward transfer by eddies sustained the strong sur-

b. Northern Hemisphere (NH)

Figure 5 shows the NH climatology of storm track activity, westerly wind speed and SST gradient. Over each of the ocean basins, a major storm track extends eastward from an intense surface baroclinic zone anchored along a subarctic frontal zone off the western boundary of the basin (Fig. 5b), where warm and cool boundary currents are confluent. In a macroscopic view, the storm track is along the boundary between subtropical and subpolar gyres. In addition, the thermal contrast between a warm boundary current (the Gulf Stream or Kuroshio) and its adjacent cooler landmass also influences the storm track activity in winter (Dickson and Namias 1976; Gulev et al. 2003). Over the North Atlantic, a belt of the surface westerlies between the Icelandic Low and

face westerlies. In a macroscopic view, the Pacific APFZ remained similar between the two winters, seemingly to keep anchoring the low-level storm track and polar-front jet (not shown).

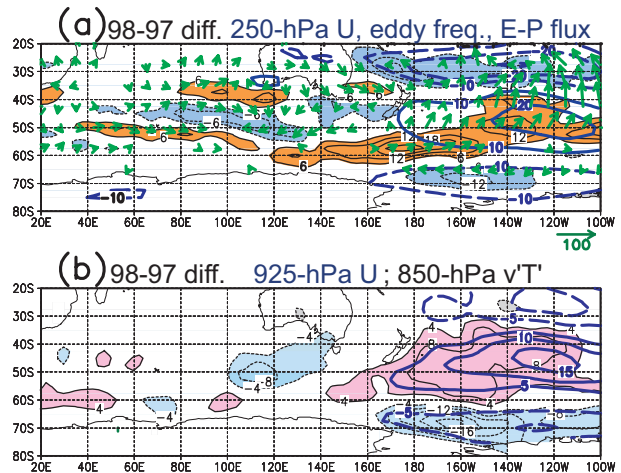


Figure 4. Difference maps over the South Indian and Pacific Oceans for Jul.-Aug. between 1997 and 1998 (1998 minus 1997). (a) Horizontal component of 250-hPa extended E-P flux (green arrows; scaling at the top; unit: $\text{m}^2 \text{s}^{-2}$) associated with subweekly eddies, 250-hPa U (blue lines for 10, 20 and 30 m s^{-1} ; dashed for anomalous easterlies) and 250-hPa storm tracks (colored). Light blue and orange coloring is applied where decrease and increase, respectively, in the frequency of an eddy amplitude maximum passing through a given data point with 2.5° intervals on a given meridian, defined as the number of days over a 62-day period, exceed 6 (thin lines for every 6). (b) 925-hPa U (blue lines for 5, 10 and 15 m s^{-1} ; dashed for the anomalous easterlies) and 850-hPa poleward eddy heat flux (K m s^{-1} ; light contours for every 4; pink and light blue for positive and negative values). Based on the NCEP reanalyses. After Nakamura et al. (2004).

Azores High is situated slightly to the south of the storm track axis. Over the wintertime North Pacific, the poleward displacement of the low-level storm track relative to the surface westerly axis is more apparent. The latter is closer to the subtropical jet axis aloft especially over the western Pacific, although the poleward secondary branch of the surface westerlies is close to the storm track.

Despite the modest intensity of the local upper-level westerly jet (Fig. 5a), midwinter storm track activity is stronger over the North Atlantic than over the North Pacific (Fig. 5b). The low-level storm track axis is closer to a subarctic frontal zone in the Atlantic than in the Pacific, and the cross-frontal SST gradient is substantially stronger in the Atlantic than in the Pacific (Fig. 5b). While its main surface axis extends along the Oyashio

Extension at $\sim 42^\circ\text{N}$, the North Pacific subarctic frontal zone at the surface is meridionally broader, including the Interfrontal Zone in the Kuroshio-Oyashio Extension (Yasuda et al. 1996; Nakamura and Kazmin 2003). The North Atlantic subarctic frontal zone is, in contrast, sharper and more intense, contributing to enhanced eddy growth and perhaps to the stronger eddy activity.

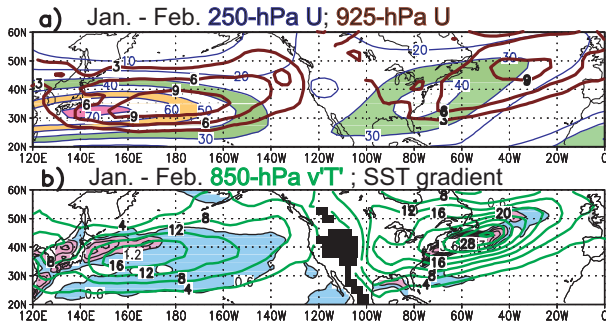


Figure 5. (a) Climatological Jan.-Feb. distribution of 925-hPa U (brown lines for every 3 m s^{-1}) and 250-hPa U (colored for $30\sim 40$ and $50\sim 60 \text{ m s}^{-1}$), based on the NCEP reanalyses. (b) As in (a) but for 850-hPa poleward eddy heat flux (green lines for every 4 K m s^{-1}). Light blue and pink shading indicates oceanic frontal zones where meridional SST gradient ($^\circ\text{C}/110 \text{ km}$) is $0.6\sim 1.2$ and above 1.2 , respectively, (with thin lines for every 0.6), based on the data by Reynolds and Smith (1994).

Another factor that contributes to the Atlantic-Pacific difference in wintertime storm track activity is latitudinal displacement between a storm track and subarctic frontal zone. In the course of its seasonal march, the North Atlantic storm track stays to the north of the subarctic frontal zone, and it is nearest to the front in midwinter when eddy activity peaks (not shown). The westerly jet axis closely follows the underlying frontal zone, especially downstream of the jet core (Fig. 5). Meanwhile, the North Pacific storm track undergoes larger seasonal migration latitudinally (Nakamura 1992; hereafter N92), and eddy activity tends to be suppressed in midwinter when the axis stays to the south of the Pacific subarctic frontal zone (Nakamura and Sampe 2002; hereafter NS02). The suppression occurs despite the fact that the mean baroclinicity peaks in midwinter.

NS02 found that upper-level eddies traveling from the Asian continent tend to propagate above the surface baroclinic zone along the frontal zone when the storm track activity peaks in spring and late fall (N92). In those seasons, the upper-level westerly jet core is substantially weaker than in midwinter and located somewhat poleward (NS02). NS02 pointed out that midwinter eddy activity has enhanced substantially since the late 1980s,

as the Pacific storm track tends to stay over the subarctic frontal zone under the decadal weakening of the subtropical jet. They found that, for most of the time during the recent midwinter periods, the eddy amplitude maximum stayed at the midlatitude tropopause right above the frontal zone (Fig. 6a), which allowed eddies efficient baroclinic growth through their interaction with a surface baroclinic zone along the frontal zone, as in fall and spring. In fact, eddies exhibited a deeper structure with vigorous poleward heat transport (Fig. 6a). In each of these situations over either the Atlantic or Pacific, the extended E-P flux is strongly divergent in the upper troposphere out of the storm track core (not shown). Thus, a westerly jet with modest core velocity bears an eddy-driven nature, a characteristic of a polar-front jet (Lee and Kim 2003). These results suggest that the association with the underlying oceanic frontal zones contributes to the enhancement of the NH storm track activity.

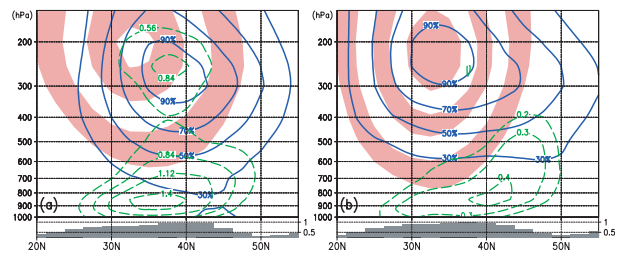


Figure 7 Meridional structure of a typical baroclinic eddy in the North Pacific storm track ($170^\circ\text{E}\sim 170^\circ\text{W}$). Based on subweekly fluctuations in geopotential height (Z) field regressed linearly on 300-hPa Z' at $[47^\circ\text{N}, 105^\circ\text{E}]$ with a 2-day lag, for (a) five Jan.-Feb. periods during 1979-95 with the weakest suppression in eddy activity and for (b) other five periods with the most distinct suppression. Reflecting the decadal weakening in the winter monsoon, the winters for (a) were all since 1987, whereas those for (b) were mostly before 1987. Eddy amplitude in Z' is normalized by its maximum (30, 50 70 and 90%). Associated poleward heat flux based on the regression (K m s^{-1} ; density adjusted) is plotted with dashed lines for 0.56, 0.84, 1.12 and 1.40 in (a) and 0.2, 0.3 and 0.4 in (b). Note that eddy amplitude is larger in (a) by 67%. The westerly jet is indicated with stippling (U : $20\sim 30$, $40\sim 50$ and $60\sim 70 \text{ m s}^{-1}$), and meridional SST gradient is plotted at the bottom ($^\circ\text{C}/110 \text{ km}$). Based on the NCEP reanalyses. After NS02.

Despite pronounced seasonal march in the axial position and intensity of the NH storm tracks, especially over the Pacific, the annually averaged surface westerly acceleration induced as the feedback forcing from the storm tracks is strongest along the poleward flank of a subarctic frontal zone over each of the ocean basins (not shown), driving oceanic gyres. In the winters of enhanced eddy activity over the Pacific (Fig. 7a), the surface westerly axis was situated along the northern fringe

of the subarctic frontal zone in the western Pacific, and it was systematically below the upper-level storm track axis over the eastern Pacific. N92 showed that, in the course of the seasonal march, the axis of the low-level westerlies tends to follow the upper-level storm track over the eastern Pacific, indicative of the reinforcement of the westerlies by the storm track.

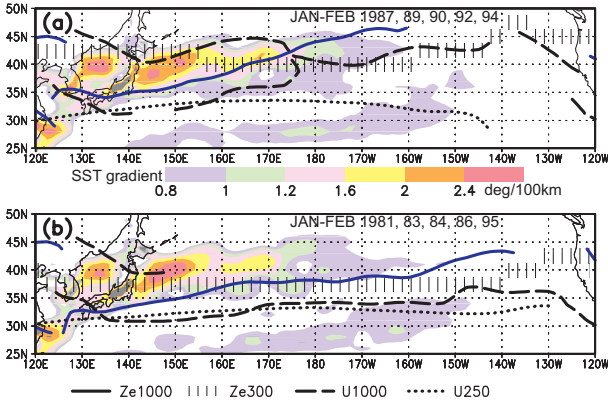


Figure 7 Relationship over the North Pacific among oceanic frontal zones (colored), storm track axes at the 1000-hPa (blue solid lines) and 300-hPa (series of vertical lines) levels, and westerly jet axes at the 1000-hPa (black dashed lines) and 250-hPa (black dotted lines) levels. For (a) five Jan.-Feb. periods in 1979-95 with the weakest suppression in eddy activity and for (b) other five periods with the most distinct suppression, as in Fig. 6. The frontal zones are indicated as regions of intense meridional SST gradient (unit: °C/110 km), as colored below (a). The storm track axes are defined as local Z_e maxima. Atmospheric and SST data are based on the NCEP reanalyses and Reynolds and Smith (1994), respectively. After Nakamura et al. (2004).

3. INFLUENCE OF A SUBTROPICAL JET ON STORM TRACK-OCEANIC FRONT ASSOCIATION

a. Southern Hemisphere (SH)

In the SH climatology (Fig. 1), the influence of the seasonal evolution of a subtropical jet stream on storm track activity is apparent only over the South Pacific (NS04). Its wintertime intensification disturbs the association among a midlatitude storm track, polar-front jet and subarctic frontal zone observed over the South Pacific in austral summer and autumn. In the presence of double-jet structure (Bals-Elsholz et al. 2001), upper-tropospheric storm track activity bifurcates from the core region into the main branch along the strong subtropical jet and the sub-branch along the weaker polar-front jet (Fig. 1a). Thus, the westerlies and storm track are no longer circumpolar. The intense velocity core of the subtropical jet confined to the tropopause (Fig. 2c) acts as an excellent waveguide for synoptic-scale eddies. In fact, the extended E-P flux associated with subweekly

eddies is consistently eastward along the jet (Fig. 1a). Located above a surface subtropical high-pressure belt, however, the jet does not favor baroclinic eddy growth, despite the modest surface baroclinicity across the underlying subtropical frontal zone (Fig. 1c). Consistently, the subtropical jet does not accompany strong westerlies at the surface (Fig. 1b), thus yielding no significant contribution to the local mechanical driving of the ocean circulation. Over the extratropical SH, the annual-mean surface westerly acceleration induced as eddy feedback forcing is weakest over the South Pacific (Fig. 3), due to the winter-spring breakdown of the well-defined midlatitude storm track. In winter and spring, the main branch of the low-level storm track is still along the polar-front jet (Figs. 1b-c), though displaced poleward above an enhanced low-level baroclinic zone that forms along the seasonal sea-ice margin (Fig. 2f). The low-level storm track forms despite the upper-level wave activity from upstream core region is mostly dispersed toward the subtropical jet (Figs. 1a and 2b), suggestive of the importance of surface baroclinicity in the storm track formation.

b. Northern Hemisphere (NH)

A factor that contributes to the Atlantic-Pacific difference in storm track activity is the midwinter eddy-activity minimum (suppression) in the North Pacific (N92). As opposed to linear theories of baroclinic instability, this unique aspect of the seasonal cycle occurs despite the local westerly jet is strongest in midwinter. Nakamura et al. (2002) found the activity minimum has disappeared since the late 1980s, under the decadal weakening of the East Asian winter monsoon and associated relaxing of the subtropical jet. In the wintertime Far East, the low-level monsoonal northerlies and the enhanced subtropical jet aloft, as observed before the late 1980s, are associated with the marked deepening of a planetary-wave trough, and a polar-front jet tends to merge itself into the subtropical jet. By the northerly component behind the trough, upper-level eddies are driven strongly toward the intensified subtropical jet and then trapped into its core at $\sim 32^\circ\text{N}$ at the 200-hPa level. The core is ~ 12 km in altitude, ~ 3 km higher than the midlatitude tropopause (300 hPa) at which eddies have been propagating through the polar-front jet over the Asian continent. In fact, the storm track underwent greater equatorward excursion from its annual-mean position in five midwinter periods with the most distinct eddy-activity minimum than in five other midwinter periods without the minimum (NS02). Trapped by the subtropical jet core, eddies were lifted up by ~ 3 km and then staying 500-800 km away from the surface baroclinic zone above the subarctic frontal zone at $\sim 40^\circ\text{N}$ (Fig. 6b). Thus, eddy interaction

with the surface baroclinic zone tended to be impaired, while eddies underwent substantial distortion in their structure. The coherency is thus lowered between sub-weekly fluctuations in temperature and meridional or vertical wind component (N92; Nakamura et al. 2002), leading to the less efficient energy conversion for eddy growth. As shown Fig. 6b, under the trapping, eddy amplitude decays rapidly downward and the associated heat flux was reduced by as much as 40%.

5. DISCUSSIONS WITH NUMERICAL EXPERIMENTS

As discussed above, the whole dynamical picture of storm tracks and polar-front jets, including the localization of their core regions, can unlikely be obtained without considering their interaction with the underlying ocean, as first argued by HV90 and recently by NS02, Inatsu et al. (2003) and NS04. In particular, key aspects of seasonal variations of a storm track can be interpreted reasonably well from a viewpoint of how strongly its association with the underlying subarctic frontal zone is disturbed by the seasonal intensification of a subtropical jet (NS02, NS04). From this viewpoint, an insight can be gained into the mechanisms that cause the “midwinter activity minimum” of the North Pacific storm track (NS02), a puzzling feature of its seasonal cycle that cannot be explained by linear theories of baroclinic instability. The recent disappearance of the activity minimum may be interpreted as the consequence of the decadal weakening in the subtropical jet. Of course, the total baroclinicity within the troposphere must be considered in interpreting the profound seasonal march in the eddy amplitude along the NH storm tracks, as discussed by HV90. They also emphasized the latent heat release along the storm tracks also acts to anchor them by forcing the planetary wave pattern.

It is well known that differential radiative heating acts to restore the mean baroclinicity at midlatitudes against the relaxing effect by eddy heat transport, but it provides no clear explanation why such intense surface baroclinic zones as observed are maintained. A tendency for major maritime surface baroclinic zones to be placed near midlatitude oceanic frontal zones (NS02; NS04) suggests the effective restoring of atmospheric baroclinicity, owing to the large thermal inertia of the ocean mixed layer and the differential thermal advection between the north and south of the frontal zones by strong oceanic currents (Kelly and Dong 2004). Enhanced heat and moisture fluxes over a warm current just south of a subarctic frontal zone has been known to contribute to cyclogenesis and thus storm track formation (HV90). In addition, a sharp decline of the surface heat release poleward across the frontal zone acts to restore the mean atmospheric near-surface baroclinicity, thus also

contributing to the anchoring of the storm track. This anchoring, however, can be disturbed by the seasonal intensification of a subtropical jet or its interannual modulations due to a teleconnection from the tropics or an upstream continent. An important scientific issue to be clarified is how the near-surface baroclinicity is determined and maintained in the marine boundary layer.

Another important aspect of the air-sea coupling associated with a storm track is that the mean westerly momentum carried downward with upward wave-activity transfer in a storm track is organized into a surface westerly jet, which drives oceanic gyres (or the ACC) and thereby contributes to the maintenance of subarctic frontal zones. Along the ACC, the core regions of the storm track, surface westerlies and APFZ almost coincide with each other, indicative of the presence of a local feedback loop. Over each of the NH ocean basins, the frontal zone is located at the confluent region of the western boundary currents driven mainly through gyre adjustment by the surface westerlies that are strongest farther to the east (Fig. 4b). A storm track acts to maintain the westerlies, especially along or slightly to the north of the subarctic frontal zones. The surface westerlies along the storm track also enhance the surface evaporation, whereas precipitation associated with migratory storms largely determines the fresh water supply to the midlatitude ocean (Lukas 2001). Kinetic energy input into the ocean by the strong surface westerlies and vigorous storm activity acts to sustain the mixed layer structure. The input also becomes an important source of oceanic turbulence available for deep-layer mixing (Nagasawa et al. 2000).

Findings in this and related papers (NS02, NS04; Nakamura et al. 2004) may require some modifications to conceptual models for the zonally symmetric circulation in the wintertime troposphere, including a well-known model by Palmén and Newton (1969). A fundamental modification we would add to the model is the possible association among a polar-front jet, storm track, surface baroclinic zone over a subarctic frontal zone, as postulated in Fig. 8a, which may add further significance to the midlatitude air-sea interaction (Nakamura et al. 2004). Unlike the polar frontal zone tilted distinctly poleward, a polar-front jet and associated baroclinic zone extend more vertically down to the surface just above the frontal zone (Fig. 2). The jet is accompanied by a major storm track, and its deep structure is a manifestation of its eddy-driven nature (Lee and Kim 2003; hereafter LM03).

Another point emphasized in Fig. 8 is their distinct characteristics between the two types of jets, as a factor that influences the observed seasonal evolution of storm tracks. In fact, two types of schematics are presented in

Fig. 8 depending upon the strength of a subtropical jet, as in LM03. As theoretically argued by Held and Hou (1980), the jet is formed through poleward transport of angular momentum by the Hadley cell, and the jet is much stronger in the winter hemisphere where the Hadley cell is stronger. Not driven by eddies, a subtropical jet may not necessarily accompany a distinct surface baroclinic zone. Indeed, the jet axis is between the subarctic and subtropical oceanic frontal zones over the North Pacific (Fig. 5). Over the SH, the jet is located above a subtropical high-pressure belt (Fig. 1) and thus unfavorable for baroclinic eddy growth. A subtropical jet is thus shallow and confined around its tight core at the high tropopause, unless merged with a polar-front as in the wintertime North Pacific associated with a planetary-wave trough.

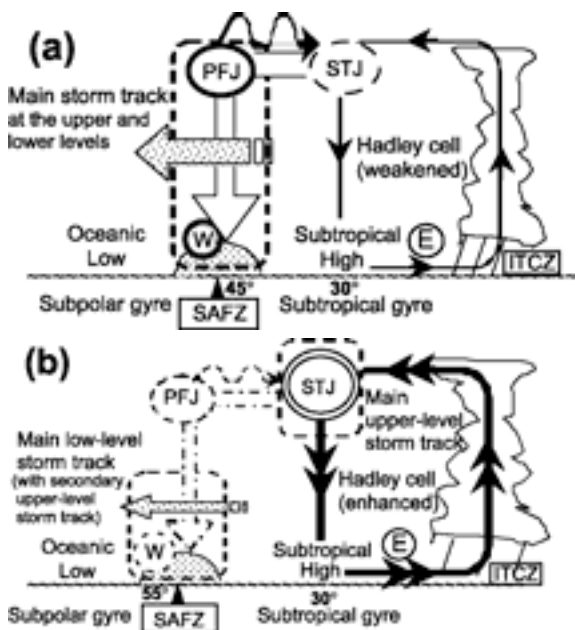


Figure 8 Schematics of different types of tropospheric general circulation over an ocean basin. (a) When a subtropical jet (STJ) is weak, the main storm track (thick dashed line) forms over a surface baroclinic zone (stippled at $\sim 45^\circ$ lat.) anchored by a subarctic frontal zone (SAFZ), as in the summertime SH, the North Atlantic or the North Pacific (in spring and fall). Wave-activity dispersion to the STJ (wavy arrow) leads to the formation of a deep polar-front jet (PFJ) above the SAFZ. Eddy downward transport (open arrow) of the mean-flow westerly momentum maintains a surface westerly jet (circled W) along the SAFZ. (b) When a STJ intensifies as in the wintertime South Pacific, the jet traps most of the upper-level eddy activity. Thus, the main branch of the upper-level storm track forms along the STJ with suppressed baroclinic eddy growth below, while the low-level storm track forms along a weak PFJ above a baroclinic zone anchored by the SAFZ.

Through idealized numerical experiments, LM03 examined how storm track activity depends on the subtropical jet intensity. They found that the main storm track forms along a polar-front jet, as in Fig. 8a, only when a subtropical jet is weak, consistent with the observations (NS02; NS04). However, the greatest discrepancy is that a subtropical jet, as it intensifies in the model, becomes increasingly favorable for baroclinic eddy growth. As opposed to their experiments, the jet intensification in the real atmosphere is unfavorable for storm track formation. Over each of the North and South Pacific, an intensified wintertime subtropical jet traps eddies into its core, keeping them away from a surface baroclinic zone anchored by a subarctic oceanic frontal zone. The trapping thus impairs eddy growth, despite the marked baroclinicity below the jet core. Over the South Pacific, where the two jets are well separated, the trapping leads to the meridional separation of the main storm track branch between the upper and lower levels [NS04]. We suggest this is a typical situation of the subtropical-jet-dominant regime (Fig. 8b). No such separation occurs over the North Pacific, where the two jets are merged. Still, the subtropical jet traps eddy activity, resulting in the midwinter suppression of storm track activity. This is an intermediate situation between the two prototype situations in Fig. 8. The storm track activity is enhanced in fall and spring when eddies can propagate above the subarctic frontal zone. This “weak subtropical-jet regime” (Fig. 8a) appears more typically over the North Atlantic and the summertime SH.

In the real atmosphere, the main storm track branch exhibits an apparent preference for staying with a polar-front jet, perhaps due to the anchoring effect by an underlying oceanic frontal zone. This preference may be underestimated in the idealized experiments by LM03. Their experiments would have been more realistic if well-defined surface baroclinic zones as observed had been prescribed. To confirm this point, we have performed a set of atmospheric general circulation model (AGCM) experiments[#] with a pair of SST distributions assigned as the model lower-boundary condition. One of them was taken from the observed SST over the Southwestern Indian Ocean as an average between 40°E and 80°E . Since we adopted a simple model setting with the entire earth surface covered by the ocean with zonally uniform SSTs, we assigned the observed SST profile for

[#]The AGCM we used is called AFES, an AGCM for the Earth Simulator, whose code was originally developed jointly by the Center for Climate System Research (CCSR), University of Tokyo and Japanese National Institute for Environmental Studies (NIES) and has been rewritten thoroughly for the best computational performance on the Earth Simulator (Singu et al. 2003; Ohfuchi et al. 2004).

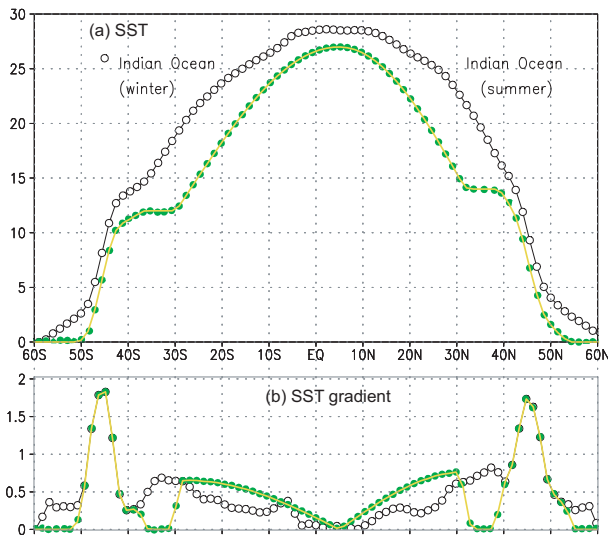


Figure 9. Meridional profiles of (a) SST ($^{\circ}\text{C}$) and (b) its gradient ($^{\circ}\text{C}/110\text{ km}$), assigned as the lower-boundary condition for AGCM experiments. The observed SST profiles for austral winter (JJA) and summer (DJF) assigned to the model SH and NH, respectively, have been connected at 3°N . The SST as an average between 40°E and 80°E was taken from the data set compiled by Reynolds and Smith (1994).

winter to the model SH and the summer profile to the model NH (as denoted by open circles in Fig. 9a). The profile is characterized by sharp SST gradient associated with the APFZ at 45°S (and at 45°N) as evident in Fig. 9b. For the other SST profile, the observed profile has been modified in such a way that it displays an unrealistically large decline from the Tropics into the subtropics (as denoted with green dots in Fig. 9) with an apparent peak at 5°N . Note that no modification has been added to the sharp SST gradient across the APFZ.

Owing to its broad peak in the Tropics, the observed SST profile yields a Hadley Cell with modest intensity. Thus, the subtropical jet has a modest core velocity (55 m/s) in the winter hemisphere (Fig. 10b). In the summer hemisphere, both a storm track and a deep polar-front jet form at midlatitudes under the diminished subtropical jet (Fig. 10a). The enhanced poleward eddy heat transport just above the near-surface baroclinic zone indicates vigorous baroclinic eddy growth occurring above the APFZ. The simulated situation is similar to what is observed over the core region of the SH storm track in summer (Fig. 1), and it is apparently in the “weak subtropical-jet regime” as shown in Fig. 8a. In the winter hemisphere, baroclinic eddy growth is the most pronounced at midlatitudes above the APFZ, in spite of enhanced mean baroclinicity below the seasonally intensified subtropical jet (Fig. 10b). In the upper tropo-

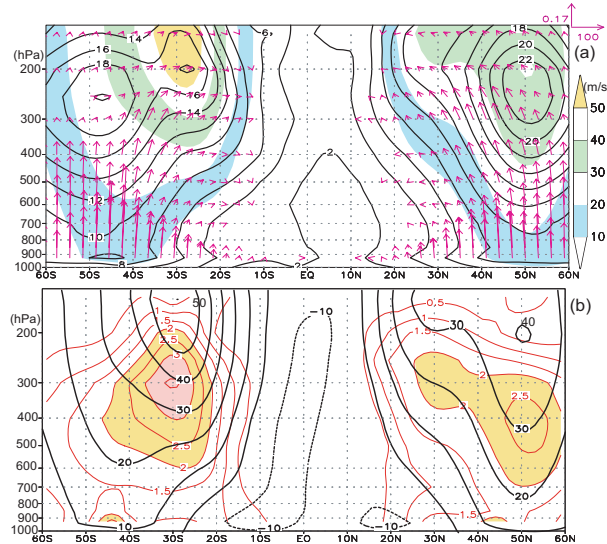


Figure 10. (a) Eddy statistics and (b) zonal mean flow simulated in an “aqua-planet” AGCM experiment with the observed SST profile (shown in Fig. 9 with open circles) assigned as the zonally uniform lower-boundary condition. The zonally averaged statistics are based on a 3-year integration. In (a), black lines denote standard deviation in meridional velocity (m/s) equivalent to eddy amplitude, and purple arrows indicate the eddy-associated Eliassen-Palm flux (with scaling at the upper-right corner). The zonal-mean westerly wind speed (m/s) is shown in (a) with coloring (as indicated to the right) and in (b) with black lines (every 10 m/s). In (b), mean-flow baroclinicity as measured by the Eady growth rate G is superimposed with red contours and coloring.

sphere, eddy activity is meridionally split to form double storm track axes, one at midlatitudes above the APFZ and the other along the subtropical jet just below its core. As observed in the wintertime SH, wave activity generated in the midlatitude low-level baroclinic zone appears to be dispersed into the subtropical jet and then trapped near the jet core. Seemingly, the trapping of wave activity leads to the slight reduction in the storm track activity relative to the summertime situation.

In a companion experiment with the modified SST profile (Fig. 9), the subtropical jet becomes enhanced with its core velocity exceeding 70 (m/s) in the winter hemisphere (Fig. 11b). The main branch of the upper-level storm track is now along the subtropical jet (Fig. 11b), with a secondary branch at 55°S , as observed in the wintertime South Pacific (Fig. 1a). Again, the baroclinic eddy growth is the most vigorous just above the midlatitude APFZ (Fig. 11a), despite the profound mid-tropospheric baroclinicity below the subtropical jet core. The enhanced eddy poleward heat flux associated with the eddy growth transports the mean-flow westerly mo-

mentum, contributing the poleward shift of the near-surface westerly jet (at $\sim 35^\circ\text{S}$) relative to the latitude of the subtropical jet core (at $\sim 30^\circ\text{S}$). The situation is similar in the summer hemisphere. In the presence of the weakened Hadley Cell, the subtropical jet also weakens shifting its core poleward (Fig. 11b), leading to the slight enhancement of the upper-level storm track activity.

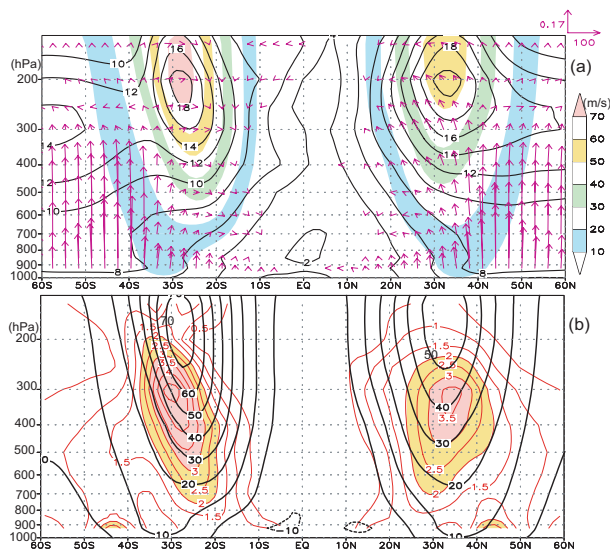


Figure 11. As in Fig. 10, but for another AGCM experiment with the modified SST profile (shown in Fig. 9 with green dots).

Of course, the schematics in Fig. 8 are nothing but a working hypothesis. Although the observational analyses and AGCM experiments presented in this paper seem to support the hypothesis, further observational and modeling study is hence needed to assess how relevant they are to extracting the essence of the atmospheric general circulation observed in the extratropics. More study is also needed to assess the robustness and detailed mechanisms of the positive feedback loop, if really exists, among a polar-front jet, storm track and subarctic frontal zone, and its importance in the climate variability. Especially, the significance of the anchoring effect by oceanic frontal zones should be confirmed in experiments with an AGCM with resolution high enough to resolve the cross-frontal thermal contrasts. It is also important to study how the oceanic fronts are maintained under the forcing from overlying storm tracks.

References

Bals-Elsholz, T. M., E. H. Atallah, L. F. Bosart, T. A. Wasula, M. J. Cempa, and A. R. Lupo, 2001: The wintertime Southern Hemisphere split jet: Structure, variability and evolution. *J.*

Climate, **14**, 4191-4215.

Berbery, E. H., and C. S. Vera, 1996: Characteristics of the Southern Hemisphere winter storm track with filtered and unfiltered data. *J. Atmos. Sci.*, **53**, 468-481.

Chang, E. K. M., 1993: Downstream development of baroclinic waves as inferred from regression analysis. *J. Atmos. Sci.*, **50**, 2038-2053.

_____, 1999: Characteristics of wave packets in the upper troposphere. Part II: Seasonal and hemispheric variations. *J. Atmos. Sci.*, **56**, 1729-1747.

_____, and D. B. Yu, 1999: Characteristics of wave packets in the upper troposphere. Part I: Northern Hemisphere winter. *J. Atmos. Sci.*, **56**, 1708-1728.

_____, S. Lee, and K. L. Swanson, 2002: Storm track dynamics. *J. Climate*, **15**, 2163-2183.

Colling, A., 2001: *Ocean Circulation, 2nd Edition*, pp. 286, The Open University, Butterworth-Heinemann, Oxford, U.K..

Dickson, R. R., and J. Namias, 1976: North American influences on the circulation and climate of the North Atlantic sector. *Mon. Wea. Rev.*, **104**, 728-744.

Gulev, G. K., T. Jung, and E. Ruprecht, 2003: Climatology and interannual variability in the intensity of synoptic-scale processes in the North Atlantic from the NCEP-NCAR reanalysis data. *J. Climate*, **15**, 809-828.

Held, I. M., and A. Y. Hou, 1980: Nonlinear axially symmetric circulations in a nearly inviscid atmosphere. *J. Atmos. Sci.*, **37**, 515-533.

Hoskins, B. J., and P. J. Valdes, 1990: On the existence of storm tracks. *J. Atmos. Sci.*, **47**, 1854-1864.

Hoskins, B. J., M. E. McIntyre, and A. W. Robertson, 1985: On the use and significance of isentropic potential vorticity maps. *Quart. J. Roy. Meteor. Soc.*, **111**, 877-946.

Inatsu, M., H. Mukougawa, and S.-P. Xie, 2003: Atmospheric response to zonal variations in mid-latitude SST: Transient and stationary eddies and their feedback. *J. Climate*, **16**, 3314-3329.

Kelly, K. A., and S. Dong, 2004: The relationship of western boundary current heat transport and storage to mid-latitude ocean-atmosphere interaction. *Ocean-Atmosphere Interactions and Climate Change*, Geophys. Monogr., Amer. Geophys. Union, in press.

Lee, S., and I. M. Held, 1993: Baroclinic wave packets in models and observations. *J. Atmos. Sci.*, **50**, 1413-1428.

_____, and H.-K. Kim, 2003: The dynamical relationship between subtropical and eddy-driven jets. *J. Atmos. Sci.*, **60**, 1490-1503.

Lukas, R. B., 2001: Freshening of the upper pycnocline in the North Pacific subtropical gyre associated with decadal changes of rainfall. *Geophys. Res. Lett.*, **28**, 3485-3488.

Nagasawa, M., Y. Niwa, and T. Hibiya, 2000: Spatial and temporal distribution of the wind-induced internal wave energy available for deep water mixing in the North Pacific. *J. Geophys. Res.*, **105**, 13933-13943.

Nakamura, H., 1992: Midwinter suppression of baroclinic wave activity in the Pacific. *J. Atmos. Sci.*, **49**, 1629-1641.

_____, and T. Sampe, 2002: Trapping of synoptic-scale disturbances into the North-Pacific subtropical jet core. *Geophys. Res. Lett.*, **29**, doi: 1029/2002GL015335.

_____, and A. S. Kazmin, 2003: Decadal changes in the North

- Pacific oceanic frontal zones as revealed in ship and satellite observations. *J. Geophys. Res.*, **108**, doi:10.1029/JC19990085.
- _____, and A. Shimpo, 2004: Seasonal variations in the Southern Hemisphere storm tracks and jet streams as revealed in a reanalysis data set. *J. Climate*, **17**, 1828-1842.
- _____, T. Izumi, and T. Sampe, 2002: Interannual and decadal modulations recently observed in the Pacific storm track activity and East Asian winter monsoon. *J. Climate*, **15**, 1855-1874.
- _____, T. Sampe, Y. Tanimoto and A. Shimpo, 2004: Observed associations among storm tracks, jet streams and midlatitude oceanic fronts. *Ocean-Atmosphere Interactions and Climate Change*, Geophys. Monogr., Amer. Geophys. Union, in press.
- Ohfuchi W., H. Nakamura, M. Yoshioka, T. Enomoto, K. Takaya, X. Peng, S. Yamane, T. Nishimura, Y. Kurihara and K. Ninomiya, 2004: 10-km mesh meso-scale resolving global simulations of the atmosphere on the Earth Simulator – Preliminary outcomes of AFES (AGCM for the Earth Simulator), *Journal of the Earth Simulator*, **1**, 8-34.
- Orlanski, I., and E. K. M. Chang, 1993: Ageostrophic geopotential fluxes in downstream and upstream development of baroclinic waves. *J. Atmos. Sci.*, **50**, 212-225.
- Palmén, E., and C. W. Newton, 1969 *Atmospheric Circulation Systems: Their Structure and Physical Interpretation*, Academic Press, New York, N.Y., 603 pp.
- Reynolds, R. W., and T. M. Smith, Improved global sea surface temperature analysis using optimum interpolation, *J. Clim.*, **7**, 929-948, 1994.
- Sanders, F., and J. R. Gyakum, 1980: Synoptic-dynamic climatology of the "bomb". *Mon. Wea. Rev.*, **108**, 1589-1606.
- Shingu, S., H. Fuchigami, M. Yamada, Y. Tsuda, M. Yoshioka, W. Ohfuchi, H. Nakamura and M. Yokokawa, 2003: Performance of the AFES: Atmospheric General Circulation Model for Earth Simulator, *Parallel Computational Fluid Dynamics – New Frontiers and Multi-Disciplinary Applications*, K. Matsuno, A. Ecer. J. Periaux, N. Satofuka and P. Fox, Eds., Elsevier, 79-86.
- Sinclair, M. R., 1995: A climatology of cyclogenesis for the Southern Hemisphere, *Mon. Wea. Rev.*, **123**, 1601-1619.
- Swanson, K. L., and R. T. Pierrehumbert, 1994: Nonlinear wave packet evolution on a baroclinically unstable jet. *J. Atmos. Sci.*, **51**, 384-396.
- Trenberth, K. E., Storm tracks in the Southern Hemisphere, *J. Atmos. Sci.*, **48**, 2159-2178, 1991.
- _____, W. G. Large and J. G. Olson, The mean annual cycle in global ocean wind stress, *J. Phys. Oceanogr.*, **20**, 1742-1760, 1990.
- Xie, S.-P., J. Hafner, Y. Tanimoto, W.T. Liu, H. Tokinaga and H. Xu, 2002: Bathymetric effect on the winter sea surface temperature and climate of the Yellow and East China Seas. *Geophys. Res. Lett.*, **29**, 3261, doi: 10.1029/2002GL015884.
- Yasuda, I., K. Okuda, and Y. Shimizu, 1996: Distribution and modification of North Pacific intermediate water in the Kuroshio-Oyashio Interfrontal Zone. *J. Phys. Oceanogr.*, **26**, 448-465.